CrystEngComm

Cite this: *CrystEngComm*, 2012, **14**, 5710–5713

www.rsc.org/crystengcomm

COMMUNICATION

A visible-light-driven solid state photo-Fenton reagent based on magnetite/carboxylate-rich carbon spheres†

Zhijun Luo,*[ac] Hongjun Tang,[b] Lingling Qu,[b] Tingting Han[b] and Xiangyang Wu*[a]

Received 27th May 2012, Accepted 18th June 2012
DOI: 10.1039/c2ce25834j

A visible-light-driven solid state photo-Fenton reagent based on magnetite/carboxylate-rich carbon spheres (MCRCSs) has been one-step fabricated *via* hydrothermal carbonization (HTC) process. Without using H_2O_2, MCRCSs exhibit excellent photodegradation activity at neutral pH under visible light irradiation.

Recently, iron-based photocatalytic systems for wastewater treatment have attracted much attention because of their low cost and benignity to environment. Among varied iron-based photocatalytic systems, the photo-Fenton reaction is one of the most efficient routes for wastewater treatment *via* hydroxyl radicals (•OH).[1] The classical homogeneous photo-Fenton system ($Fe^{3+}/H_2O_2/UV$) has some intrinsic drawbacks that limit its widespread application, such as a narrow working pH range, high H_2O_2 dosage, and difficulty of separation and recovery of the iron species.[2] Iron oxides as catalysts, the solidification of iron ions, and H_2O_2 together under light irradiation could set up a heterogeneous photo-Fenton system, which can destroy organic pollutants efficiently in a wider pH range with much less iron loss than the homogeneous photo-Fenton system.[3] Without using unstabilized H_2O_2, another interesting photo-Fenton system is the combination of carboxylic acids (such as oxalic, malic, citric, tartaric acids, *etc.*) and iron (just dissolved or as oxides), which can form ferricarboxylate complexes that absorb light irradiation with high quantum yield to trigger radical chain mechanisms of oxidation.[4] If the carboxylic acids can be solidified just like the solidification of iron ions, it is feasible to fabricate the solid state photo-Fenton reagent through the solidification of iron ions and carboxylic acids at the same time, which is different from the homogeneous and heterogeneous photo-Fenton reagent.

Compared with the intensive research of fullerenes, carbon nanotubes (CNTs), and graphene, amorphous carbon, another allotrope of carbon, has been neglected in photocatalytic applications.[5] The merit of amorphous carbon obtained by a hydrothermal carbonization (HTC) process is that rich functional groups can be retained, which can greatly improve hydrophilicity and chemical reactivity.[6] However, the amount of carboxylic acid groups contained in amorphous carbon obtained by HTC is rather low, underlining the highly reductive conditions throughout the hydrothermal, oxygen-free carbonization reaction (the constituting aldoses transform into aldehydes onto the surface), which makes it difficult to obtain the carboxylate-rich carbon materials.[7] Titirici *et al.* reported that carboxylate-rich carbon could be obtained *via* the cycloaddition reaction between acrylic acid and glucose during the HTC process.[8]

The motivation of the present research derived from the idea that encapsulating Fe_3O_4 particles with an amorphous carbon sphere rich in carboxylate groups can form ferricarboxylate complexes, which can yield •OH under visible light irradiation. Herein, we report a facile one-step route to directly fabricate MCRCSs. Without using H_2O_2, MCRCSs exhibit excellent photodegradation activity for methylene blue (MB) at neutral pH under visible light irradiation. In addition, it own unique superiority in separation and recycling allows it to be collected easily by applying an appropriate magnetic field. To the best of our knowledge, this is the first report about the visible-light-driven solid state photo-Fenton reagent based on MCRCSs.

Generally, the fabrication of Fe_3O_4/carbon composites require two steps, the synthesis of an Fe_3O_4 core and the subsequent coating of the carbon shell, which makes the synthesis route complicated and render the catalysts too expensive for widespread industrial use.[9] In the present study, we develop a facile one-step synthesis of MCRCSs, which only needs two reagents: the single iron source $FeCl_3$ and sodium gluconate. Different functional groups of sodium gluconate play synergetic roles in the formation of MCRCSs as illustrated in Scheme 1: (1) the hydrolysis of sodium gluconate, which is the strong base–weak acid salt, provides controlled quantities of OH^- ions for the formation of Fe_3O_4; (2) Fe^{3+} can be reduced into Fe^{2+} in the presence of large numbers of reductive hydroxyl groups of sodium gluconate under the hydrothermal treatment; (3) sodium gluconate as the derivative of glucose could form the carboxylate-rich carbon *via* the aromatization and carbonization reaction during the HTC process. In addition, the strong coordinating ability of carboxylate group to metal cations means the gluconate can strongly bond with the Fe atom of surface of Fe_3O_4 particles, which is propitious to the *in situ* carbon coating on Fe_3O_4 particles.

[a]*School of The Environment, Jiangsu University, Zhenjiang, 212013, P. R. China. E-mail: lzj@ujs.edu.cn*
[b]*School of Chemistry and Chemical Engineering, Jiangsu University, Zhenjiang, 212013, P. R. China*
[c]*State Key Laboratory of Coordination Chemistry, Nanjing University, Nanjing, 210093, P. R. China*
† Electronic supplementary information (ESI) available. See DOI: 10.1039/c2ce25834j

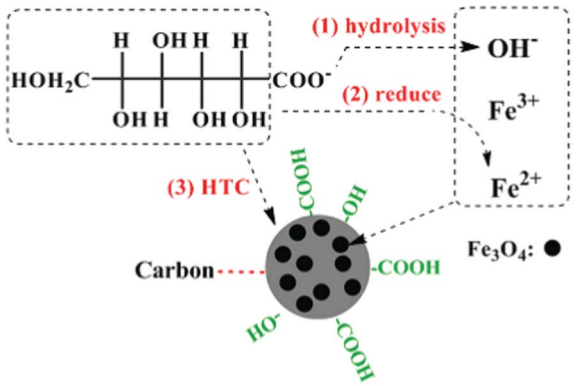

Scheme 1 Functional groups of sodium gluconate play synergetic roles in the formation of MCRCSs.

The XRD pattern (Fig. 1a) of the as-prepared samples could be indexed as *Fd3m* cubic Fe_3O_4 (JCPDS card No. 11-0614). No other characteristic peaks such as the impurities of hematite or hydroxides were detected, suggesting high purity of the as-synthesized Fe_3O_4 in MCRCSs. No obvious diffraction peak for the carbon is observed, suggesting the carboxylate-rich carbon is amorphous carbon. The Raman spectra (Fig. 1b) for MCRCSs shows the characteristic wide D and G bands around 1360 and 1580 cm^{-1}, respectively, typical for amorphous carbons. The large I_D/I_G value (0.8) indicates the low degree of graphitization of the carboxylate-rich carbon. The carbon content is determined by thermogravimetric analysis (TGA, Fig. S1†). It can be noticed that the weight loss below 190 °C could probably be attributed to the evaporation of the adsorbed moisture or gaseous molecules, and the major weight loss takes between 190 °C and 450 °C, giving rise to a large weight loss of about 59.28 wt%. While considering that Fe_3O_4 will be converted into Fe_2O_3 when heated in air, the actual carbon content in the MCRCSs can be estimated to be about 64.16%. Fig. 1c presents a panoramic scanning electron microscopy (SEM) image of the MCRCSs. It can be seen that the MCRCSs have a relatively uniform diameter of about 5 μm. The high-resolution SEM image of an individual sphere (Fig. 1d) shows that these spheres are constructed of numerous particles.

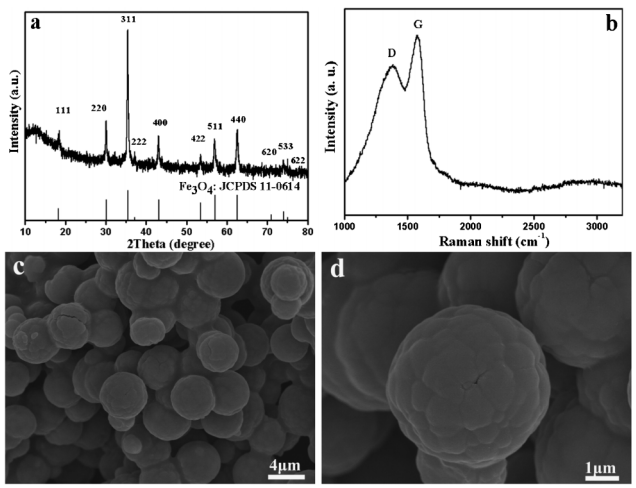

Fig. 1 (a) XRD pattern, (b) Raman spectrum, and (c and d) SEM images of MCRCSs.

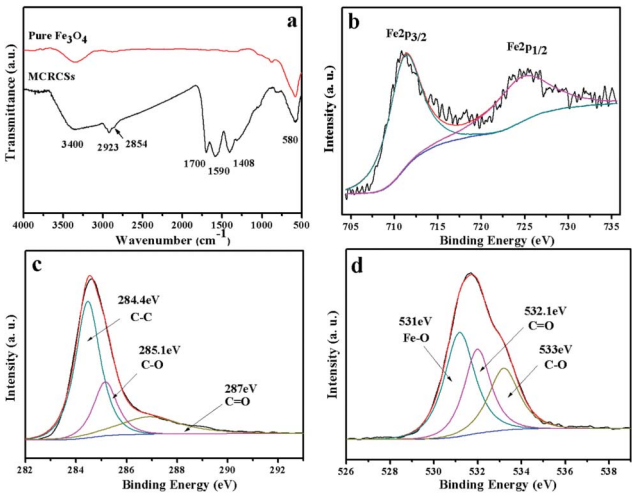

Fig. 2 FT-IR and XPS spectra of MCRCSs: (a) FT-IR, (b) Fe 2p, (c) C 1s, (d) O 1s.

FT-IR spectroscopy was further used to investigate the functional groups remaining on the surface of MCRCSs. For the purpose of comparing MCRCSs with Fe_3O_4 nanoparticles, Fe_3O_4 nanoparticles were synthesized and the XRD pattern and TEM image are shown in Fig. S2 and Fig. S3,† respectively. Fig. 2a shows the FT-IR spectra curves of Fe_3O_4 nanoparticles and MCRCSs. The band at 1700 cm^{-1} is associated with carbonyl in carboxylate group.[8] Two additional vibration bands located at 1590 and 1408 cm^{-1} can be assigned to the asymmetric and symmetric stretching vibration of COO^- groups, confirming that large amounts of carboxylate groups from carbon were coordinated strongly to the iron cations.[10] The band at 580 cm^{-1} is attributed to the Fe–O stretch, which indicates the existence of Fe_3O_4.[11] The bands at 3400 cm^{-1} imply the existence of large numbers of hydroxyl groups. The bands at 2923 and 2854 cm^{-1} should be attributed to the stretching vibration of $–CH_2–$.[10,12]

Surface analysis of the MCRCSs was carried out using X-ray photoelectron spectroscopy (XPS). In the partial XPS spectrum of Fe 2p (Fig. 2b), the peaks for Fe 2p3/2 and Fe 2p1/2 were observed at 711.2 and 724.5 eV, which is also indicative of the formation of a Fe_3O_4 phase in MCRCSs. The partial XPS spectrum of C1s (Fig. 2c) can be deconvoluted into three component peaks with binding energies at about 284.4, 285.1 and 287 eV, which are attributed to the C–C, C–O, and C=O bonds, respectively.[13] For the O 1s spectrum represented in Fig. 2d, three component peaks with binding energies at about 531, 532.1 and 533 eV were identified. They are attributed to the Fe–O, C=O, and C–O bonds, respectively.[12,13] According to the FT-IR and XPS spectra results, it was demonstrated that a large number of carboxylate groups and hydroxyl groups remained in the MCRCSs and carboxylate groups from carbon were coordinated strongly to the iron cations. As is well known, Fe_3O_4 nanoparticles are usually hydrophobic, which limits their application in the photocatalytic degradation of organic pollutants. However, these hydrophilic groups, carboxylate groups and hydroxyl groups, can endow the MCRCSs with excellent aqueous dispersibility (videos S1 and S2, ESI†).

To shed light on the formation mechanism of MCRCSs, the time-dependent experiments were carried out. Fig. S4† shows SEM images of the samples obtained during the HTC at 3 h, 6 h,

12 h, and 48 h. Fig. S4a† shows the morphology of the products obtained at 3 h, the product was mainly microspheres composed of particles and the diameter of microspheres is about 3.5 μm. These particles have a diameter of hundreds of nanometers. These particles were analyzed by energy dispersive X-ray spectroscopy (EDS). The result shown in Fig. S5† reveals that only the elements of Fe, C, and O are contained in the particles, which suggests that these particles were the Fe_3O_4/carbon composites. Microspheres composed of particles were not the exclusive morphology in the products. From the Fig. S4b,† we can clearly observe that agglomerated particles were encapsulated with carbon spheres. When the reaction time was prolonged to 6 h, more Fe_3O_4/carbon particles integrated into microspheres and most of microspheres grow, in which the diameter of microspheres increased to about 4 μm (Fig. S4c and d†). After 12 h of reaction, these microspheres composed of Fe_3O_4/carbon particles were gradually coated by carbon (Fig. S4e and f†). The diameter of Fe_3O_4/carbon microspheres did not increase but the rough surface of Fe_3O_4/carbon microspheres become smooth (Fig. S4f†). After hydrothermal treatment for 48 h, large numbers of MCRCSs were obtained and Fe_3O_4 particles were enwrapped by carbon more compactly as uniform microspheres (Fig. S4g and h†). EDS analysis on the Fe_3O_4/carbon microspheres obtained at 48 h suggests that only the elements of Fe, C, and O are contained in the microspheres (Fig. S5†). However, the intensity of C element on the surface of MCRCSs obtained at 48 h is higher than that of Fe_3O_4/carbon composites obtained at 3 h, which implies that the carbon content of product obtained at 48 h is larger than that of product obtained at 3 h.

On the basis of the information we have gathered, the synthetic strategy of MCRCSs is shown in Scheme S1.† A two stage growth mechanism of MCRCSs has been proposed. The formation of the MCRCSs is divided into two growth stages, *i.e.*, the formation of the Fe_3O_4/carbon microsphere and the further carbon coating process. In the former stage, there is a hydrolysis equilibrium of sodium gluconate in water, which provides OH^- ions for the formation of Fe_3O_4 particles. In addition, *in situ* carbon coating on Fe_3O_4 particle occurs, due to carboxylate group of sodium gluconate strongly coordinating to the Fe atom and HTC process of sodium gluconate. Then these Fe_3O_4/carbon particles agglomerate and coalesce together to form Fe_3O_4/carbon microspheres. The latter stage is the further carbon coating process, Fe_3O_4/carbon microsphere composed of Fe_3O_4/carbon particles were further enwrapped by carbon to form MCRCSs.

The visible light photocatalytic activity of MCRCSs was evaluated with the photodegradation of MB in aqueous solution at room temperature. The UV-vis spectra of MB aqueous solution with MCRCSs under visible light irradiation ($\lambda > 420$ nm) at room temperature for different durations are shown in Fig. 3a. The main absorption peak located at 665 nm, which corresponds to the MB molecule, decreases rapidly with extension of the exposure time, and was almost completely disappeared after 4 h of visible light irradiation. Further experiments were carried out to compare the photocatalytic activities of pure Fe_3O_4 nanoparticles with MCRCSs. Fig. 3b shows the curves of the degradation efficiency with irradiation time. As can be seen, without any catalyst or with pure Fe_3O_4 nanoparticles, nearly no degradation of MB was detected under visible light irradiation. However, in the

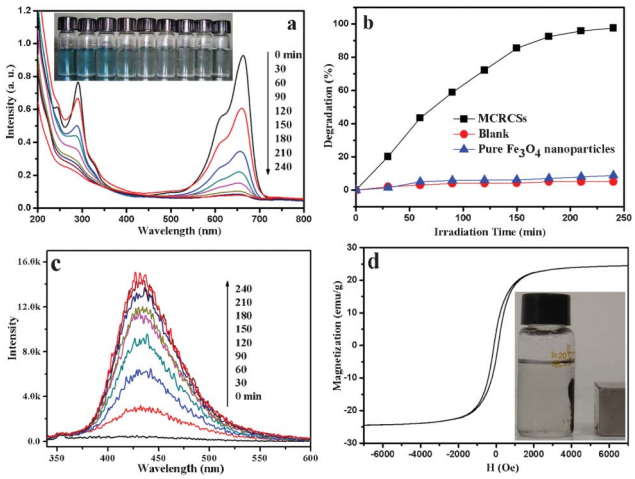

Fig. 3 (a) UV-vis spectra of MB *vs.* photoreaction time; (b) photodegradation of MB over blank, pure Fe_3O_4 nanoparticles, and MCRCSs; (c) $^{\bullet}OH$-trapping PL spectra of Fe_3O_4/carboxylate-rich carbon microspheres/TA solution; (d) field-dependent magnetization curve of Fe_3O_4/carboxylate-rich carbon microspheres at room temperature, inset shows the strong attraction of the particles suspended in water toward a magnet.

presence of MCRCSs, MB degradation reaches about 96% after 4 h of visible light irradiation without using H_2O_2.

The hydroxyl radical ($^{\bullet}OH$) has been considered as a key species in the photodegradation of many hazardous chemical compounds for its high reaction ability to attack any organic molecule. Terephthalic acid photoluminescence probing technique (TAPL), a highly sensitive and simple method, has been widely used in detection of $^{\bullet}OH$.[3b,14] The terephthalic acid (TA) probed $^{\bullet}OH$ to form 2-hydroxylterepthalic acid (HTA) during the photocatalytic process, which was measured with a fluorescence spectrophotometer. The HTA exhibited a strong fluorescence peak (λ_{ex} = 315 nm, λ_{em} = 426 nm). Thus, we measured the fluorescence intensity of HTA to detect $^{\bullet}OH$ indirectly. The photoluminescence spectra of MCRCSs–TA solution under visible light irradiation is shown in Fig. 3c. The photoluminescence peak of HTA (λ_{em} = 426 nm) increased steadily with the irradiation time, suggesting that the $^{\bullet}OH$ increased steadily, which elucidated that $^{\bullet}OH$ on MCRCSs was produced under visible light irradiation without using H_2O_2. After the photo-Fenton reaction ended, the MCRCSs could be rapidly separated under an applied magnetic field. As shown, the MCRCSs are strongly attracted to a permanent magnet (inset in Fig. 3d). The magnetic properties of MCRCSs were studied by using a superconducting quantum interference device (SQUID) magnetometer at room temperature. Fig. 3d displays hysteresis loops of MCRCSs, which indicates it possess magnetic saturation (M_s) values of about 25 emu g^{-1}.

In summary, we demonstrate a feasible, economical and green synthetic route for the synthesis of highly water-dispersible MCRCSs. The solidification of iron ions and carboxylic acids at the same time was realized *via* the fabrication of MCRCSs. Carboxylates in the amorphous carbon can form complexes with Fe_3O_4, which can produce $^{\bullet}OH$ under visible light irradiation. Therefore, without using H_2O_2, MCRCSs possess significantly enhanced photocatalytic activity under visible light irradiation and can be conveniently separated by using an applied magnetic field.

Acknowledgements

This work was supported by the Universities Natural Science Foundation of Jiangsu Province (11KJB480001), Postdoctoral Foundation of Jiangsu Province (1102125C), Jiangsu Natural Science Fund of China (SBK201222389), and Highly Qualified Professional Initial Funding of Jiangsu University (10JDG120).

References

1 (*a*) B. Ahmed, E. Limem, A. A. Wahab and B. Nasr, *Ind. Eng. Chem. Res.*, 2011, **50**, 6673–6680; (*b*) N. Klamerth, S. Malato, A. Agüera, A. F. Alba and G. Mailhot, *Environ. Sci. Technol.*, 2012, **46**, 2885–2892.

2 (*a*) A. W. Vermilyea and B. M. Voelker, *Environ. Sci. Technol.*, 2009, **43**, 6927–6933; (*b*) O. A. Makhotkina, S. V. Preis and E. V. Parkhomchuk, *Appl. Catal. B: Environ.*, 2008, **84**, 821–826.

3 (*a*) X. M. Zhou, H. C. Yang, C. X. Wang, X. B. Mao, Y. S. Wang, Y. L. Yang and G. Liu, *J. Phys. Chem. C*, 2010, **114**, 17051–17061; (*b*) G. K. Zhang, Y. Y. Gao, Y. L. Zhang and Y. D. Guo, *Environ. Sci. Technol.*, 2010, **44**, 6384–6389; (*c*) X. M. Zhou, J. Y. Lan, G. Liu, K. Deng, Y. L. Yang, G. J. Nie, J. G. Yu and L. J. Zhi, *Angew. Chem., Int. Ed.*, 2012, **51**, 178–182.

4 (*a*) F. B. Li, X. Z. Li, C. S. Liu, X. M. Li and T. X. Liu, *Ind. Eng. Chem. Res.*, 2007, **46**, 781–787; (*b*) P. Mazellier and B. Sulzberger, *Environ. Sci. Technol.*, 2001, **35**, 3314–3320; (*c*) Q. Lan, F. B. Li, C. S. Liu and X. Z. Li, *Environ. Sci. Technol.*, 2008, **42**, 7918–7923; (*d*) E. Rodríguez, G. Fernández, B. Ledesma, P. Álvarez and F. J. Beltrán, *Appl. Catal. B: Environ.*, 2009, **92**, 240–249.

5 R. Leary and A. Westwood, *Carbon*, 2011, **49**, 741–772.

6 (*a*) B. Hu, S. H. Yu, K. Wang, L. Liu and X. W. Xu, *Dalton Trans.*, 2008, 5414–5423; (*b*) B. Hu, K. Wang, L. H. Wu, S. H. Yu, M. Antonietti and M. M. Titirici, *Adv. Mater.*, 2010, **22**, 813–828.

7 M. M. Titirici, A. Thomas, S. H. Yu, J. Müller and M. Antonietti, *Chem. Mater.*, 2007, **19**, 4205–4212.

8 R. D. Cakan, N. Baccile, M. Antonietti and M. M. Titirici, *Chem. Mater.*, 2009, **21**, 484–490.

9 (*a*) X. M. Sun, J. F. Liu and Y. D. Li, *Chem. Mater.*, 2006, **18**, 3486–3494; (*b*) S. K. Li, F. Z. Huang, Y. Wang, Y. H. Shen, L. G. Qiu, A. J. Xie and S. J. Xu, *J. Mater. Chem.*, 2011, **21**, 7459–7466.

10 P. S. Yuan, Q. S. Wu, Y. P. Ding, H. Q. Wu and X. C. Yang, *Carbon*, 2009, **47**, 2648–2654.

11 Y. Liu, Z. Y. Ren, Y. L. Wei, B. J. Jiang, S. S. Feng, L. Y. Zhang, W. B. Zhang and H. G. Fu, *J. Mater. Chem.*, 2010, **20**, 4802–4808.

12 M. Sevilla and A. B. Fuertes, *Chem.–Eur. J.*, 2009, **15**, 4195–4203.

13 H. M.Sun, L. Y. Cao and L. H. Lu, *Nano Res.*, 2011, **4**, 550–562.

14 H. J. Huang, D. Z. Li, Q. Lin, W. J. Zhang, Y. Shao, Y. B. Chen, M. Sun and X. Z. Fu, *Environ. Sci. Technol.*, 2009, **43**, 4164–4168.